

Molecular Pivot-Hinge Installation to Evolve Topology in Rare-Earth Metal–Organic Frameworks

Liang Feng⁺, Yutong Wang⁺, Kai Zhang, Kun-Yu Wang, Weidong Fan, Xiaokang Wang, Joshua A. Powell, Bingbing Guo, Fangna Dai, Liangliang Zhang, Rongming Wang, Daofeng Sun,^{*} and Hong-Cai Zhou^{*}

Abstract: Linker desymmetrization has been witnessed as a powerful design strategy for the discovery of highly connected metal–organic frameworks (MOFs) with unprecedented topologies. Herein, we introduce molecular pivot-hinge installation as a linker desymmetrization strategy to evolve the topology of highly connected rare-earth (RE) MOFs, where a pivot group is placed in the center of a linker similar to a hinge. By tuning the composition of pivot groups and steric hindrances of the substituents on various linker rotamers, MOFs with various topologies can be obtained. The combination of $L-SO_2$ with C_{2v} symmetry and 12-connected RE_9 clusters leads to the formation of a fascinating (4,12)-c **dfs** new topology. Interestingly, when replacing $L-SO_2$ with a tetrahedral linker $L-O$, the stacking behaviors of RE-organic layers switch from an eclipsed mode to a staggered stacking mode, leading to the discovery of an intriguing **hjk** topology. Additionally, the combination of the RE cluster and a linker $[(L-(CH_3)_6)]$ with more bulky groups gives rise to a **flu** topology with a new 8-c inorganic cluster. The diversity of these RE-MOFs was further enhanced through post-synthetic installation of linkers with various functional groups. Functionalization of each linker with acidic and basic units in the mesoporous RE-based PCN-905- SO_2 allows for efficient cascade catalytic transformation within the functionalized channels.

Introduction

Metal–organic frameworks (MOFs), as a well-developed class of porous crystalline materials, epitomize a highly tunable structure through judicious linker design and cluster selection.^[1–9] The formation of metal clusters with selected connectivity and nuclearity can be observed during the construction of MOF structures, for example, 4-, 6-, 8-, 10-, 11- and 12-connected Zr_6 and Zr_{12} clusters can be observed in various Zr-MOFs, however, the formation of these inorganic clusters is highly dependent on the geometry, length and

connectivity of building organic linkers.^[10,11] Therefore, rational linker design is critical to expand the diversity and properties of MOFs with targeted properties and applications.

Among ditopic, tritopic, tetratopic, hexatopic and octatopic carboxylate linkers commonly used for MOF construction, tetratopic carboxylate linkers have been of a prime interest in recent years because of their highly tunable geometries and shapes.^[12] Both Zhou's and Yaghi's groups have reported the synthesis of Zr-MOFs based on a tetratopic linker tetrakis(4-carboxyphenyl)porphyrin (TCPP) with a square shape (Figure 1 a).^[13,14] The resulting materials show very diverse topologies, including **ftw**, **csq**, **shp**, **scu**, **she**, and **sqc**, due to the dynamic connection between Zr_6 clusters with varying connectivities and 4-connected TCPP linkers. Desymmetrizing the square TCPP linker into a pyrene-based ligand with rectangle shape leads to the formation of mesoporous NU-1000 with **csq** topology, similar to the PCN-222 structure (Figure 1 b).^[15] The structural tunability can be further enhanced by desymmetrization from the rectangular linker to a trapezoidal linker, where a defective MOF can be created with three crystallographically distinct pockets (Figure 1 d).^[16,17]

Alternatively, the effects of linker geometry and flexibility controlled by the bulkiness of functional groups can be utilized to enhance the diversity of highly connected MOFs. For example, by altering the positions of linker substituents, the formation of Zr-tetratopic carboxylate MOFs with various topologies can be controlled (Figure 1 c).^[18] Recently we also reported that by utilizing more adaptable rare-earth (RE) clusters, more diverse structures and topologies can be easily obtained through continuous hindrance control.^[19] Yet in all the aforementioned highly connected MOF examples, the structural diversity, flexibility and the resulting component tunability are highly limited by the rigid ligand backbone. Consequently, the enhancement of structural control over the multi-level assembly of sophisticated porous MOFs with high

[*] Y. Wang,^[†] K. Zhang, W. Fan, X. Wang, B. Guo, Dr. F. Dai, Dr. R. Wang, Prof. Dr. D. Sun
College of Science, School of Materials Science and Engineering,
China University of Petroleum (East China)
Qingdao, Shandong 266580 (China)
E-mail: dfsun@upc.edu.cn

L. Feng,^[†] K.-Y. Wang, J. A. Powell, Prof. Dr. H.-C. Zhou
Department of Chemistry, Texas A&M University
College Station, TX 77843 (USA)
E-mail: zhou@chem.tamu.edu

Prof. Dr. H.-C. Zhou
Department of Materials Science and Engineering, Texas A&M
University, College Station, Texas 77843-3003 (USA)

Dr. L. Zhang
Xi'an Institute of Flexible Electronics, Northwestern Polytechnical
University, Xi'an 710072 (China)

[†] These authors contributed equally to this work.

Supporting information and the ORCID identification number(s) for the author(s) of this article can be found under <https://doi.org/10.1002/anie.201910717>.

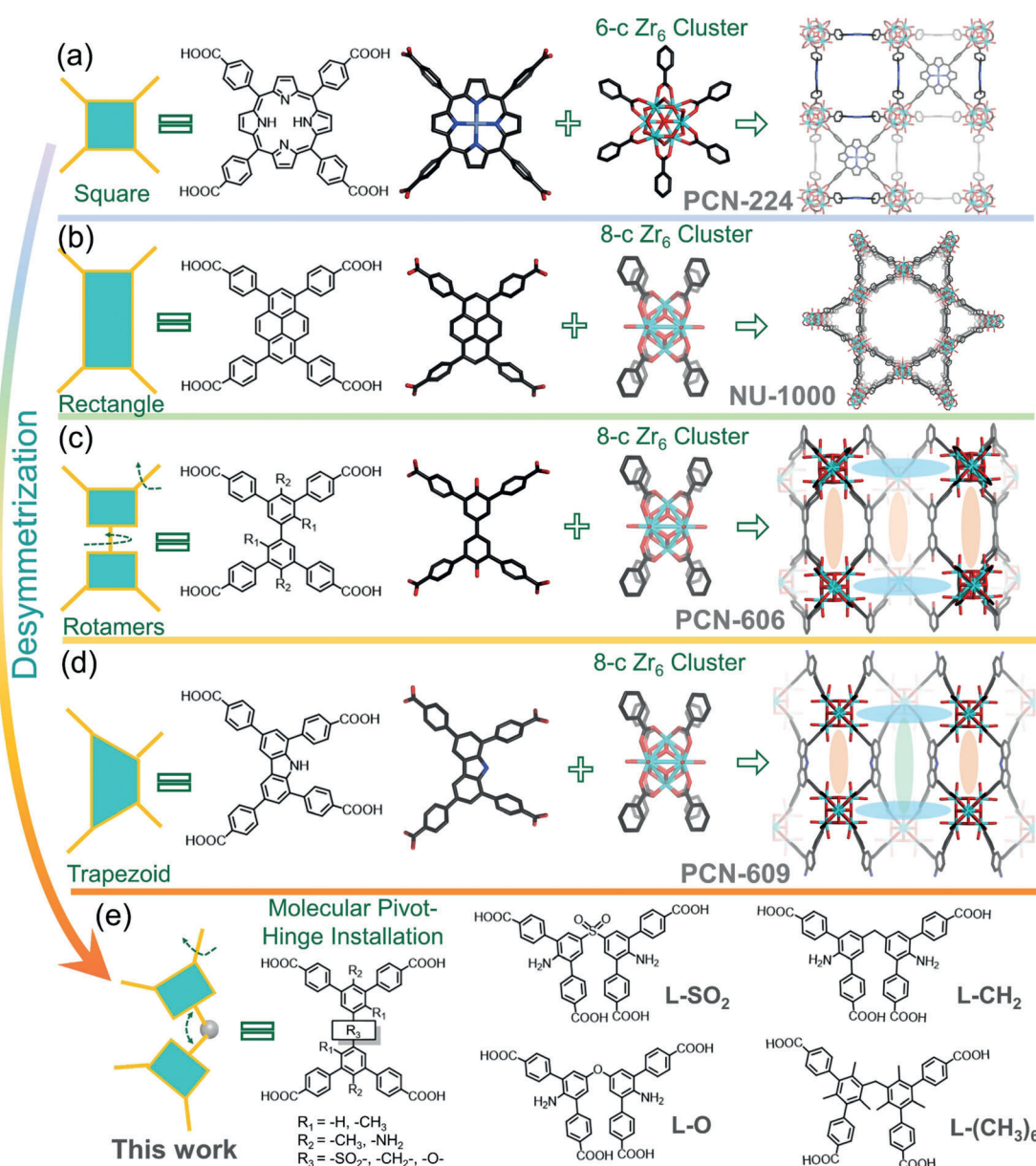


Figure 1. Illustration of the desymmetrization concept in the topology discovery of highly connected MOFs based on different linker symmetries: a) 4-c square porphyrinic linkers are linked to 6-c Zr_6 clusters into PCN-224. b) The linking of 4-c rectangle pyrene linkers with 8-connected Zr_6 clusters leads to the formation of NU-1000. c) Employment of rotamers with various steric hindrances prompted the formation of a series of MOFs with various topologies; d) Use of a trapezoidal ligand resulted in the discovery of PCN-609 reported with three different pockets for installation; e) Introduction of molecular pivot groups (R_3) and substituents (R_1 and R_2) into rotamers can induce the formation of a series of novel flexible topologies. Zr, C, O and N atoms are represented by turquoise, black, red and blue, respectively, and H atoms are omitted for clarity.

connectivities require new design concepts and guidelines. Herein, we introduce a powerful strategy, molecular pivot-hinge installation, to tailor topology and diversity in MOFs by placing a pivot group in the center of a linker similar to a hinge (Figure 1e).^[20] This joint pivot provides tunable flexibility for the two dangling hinges, allowing for the formation of ligands with various geometries and conformations. By tuning the composition of pivot groups and steric hindrances of the substituents on various linker rotamers, MOFs with various topologies can be obtained. For example, the linker L-SO₂ with SO₂ as a pivot group with C_{2v} symmetry

exhibits a 104.3° dihedral angle between the two central 6-membered rings, while the tetrahedral linker L-O with O as a pivot group has a 119.2° dihedral angle and results in an entirely different topology. Herein, we choose RE based MOFs as suitable candidates for the construction of novel topologies due to the multiple directionality of RE clusters. The combination of L-SO₂ and 12-connected RE₉ clusters leads to the formation of a new fascinating (4,12)-c **dfs** topology. The isorecticular structure of PCN-905-SO₂ can also be obtained when the RE₉ clusters were connected to a similar ligand (L-CH₂) with CH₂ as a pivot group. When replacing L-



SO₂ with the aforementioned tetrahedral linker L-O, the stacking behaviors of RE-organic layers switched from an eclipsed mode to a staggered stacking mode, leading to the discovery of a fascinating **h₁₂j₃** topology. In addition, the combination of the RE cluster and a linker [(L-(CH₃)₆)] with more bulky groups gives rise to a **flu** topology with a new 8-c inorganic cluster. The diversity of these RE-MOFs was further enhanced through post-synthetic installation of linkers with various functional groups. The open pockets in PCN-905-SO₂ enables the precise placement of functional groups within a multivariate pore environment. The installation of various linkers also leads to tunable torsion angles around the pivot groups, and the dihedral angles between the central phenyl ring and the peripheral ring. Functionalization of each linker with acidic units and base units in the mesoporous RE-based PCN-905-SO₂ allows for efficient cascade catalytic transformation within the functionalized channels. This work provides novel design strategies for the systematic design and construction of unprecedented topologies through molecular pivot-hinge installation, which shall further serve as blueprints for the discovery of highly complicate porous structures for future sophisticated applications.

Results and Discussion

Design, Synthesis and Structural Description

Herein we selected four tetratopic ligands with various molecular pivot groups (R₃) and substituents (R₁ and R₂) to construct RE-MOFs that exhibit multiple unprecedented topologies (R₁=-H, -CH₃; R₂=-NH₂, -CH₃; R₃=-SO₂-, -CH₂-, -O-). As shown in Figure 1e, the molecular pivot groups with varying rotation degrees are introduced at the linker center, tuning the rotation of the two dangling hinges around the central pivot. Meanwhile, the functional groups with various levels of steric hindrance are placed at the R₁ and R₂ position, tuning the rotation of two peripheral phenyl rings near the central one.

Solvothermal reactions between L-SO₂ and Eu-(NO₃)₃·6H₂O in the presence of 2-fluorobenzoic acid (2-FBA) for 24 h yielded large colorless crystals with cuboid morphology, PCN-905-SO₂ (also named UPC-905-SO₂, Figure 2a). The modulator, 2-FBA, can induce the in situ formation of polynuclear RE clusters (RE₆ or RE₉), which can further be utilized for the construction of extended MOFs.^[21] The formula of PCN-905-SO₂ was determined by single-crystal X-ray diffraction and the phase purity of the aforementioned products was accessed by powder X-ray diffraction (PXRD) patterns (Figure S19). Additionally, under the same condition, the reaction between Eu-(NO₃)₃·6H₂O and L-CH₂ yields large cuboid crystals with the same topology, because of the similar conformations and geometries of L-SO₂ and L-CH₂ (Figure 2b).

PCN-905-SO₂ represents a rare RE-MOF with mesoporosity and flexibility. PCN-905-SO₂ crystallized in the hexagonal space group *P6/mmm* (Table S1). Crystallographically, it contains a 12-connected RE₉ cluster [RE₉(μ₃-OH)₁₂(μ₃-O)₂(O₂C-)₁₂] and a bent tetratopic linker with C_{2v}

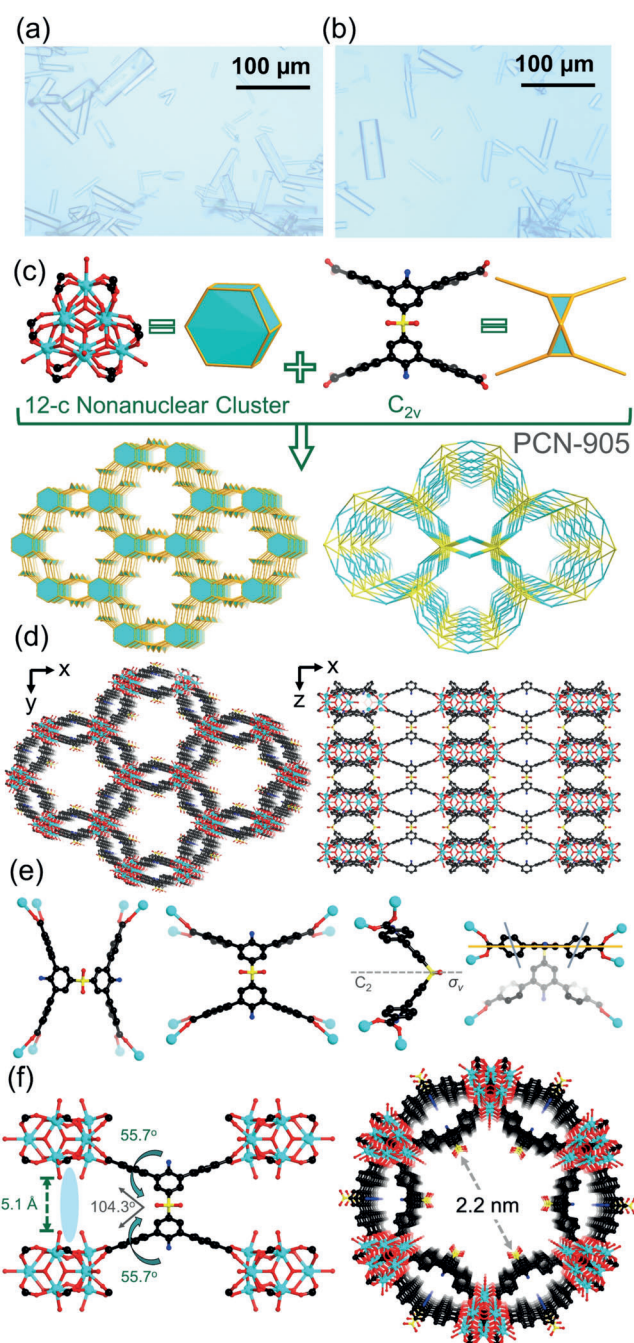


Figure 2. Structural illustration of PCN-905-SO₂ with (4, 12)-c **dfs** topology. a,b) Optical images of PCN-905-SO₂ (a) and PCN-905-CH₂ (b) single crystals. c) The assembly of 12-c RE₉ clusters and 4-c ligands with a SO₂ pivot substituent (C_{2v}) into a (4, 12)-c **dfs** net. d) The structural illustration of PCN-905-SO₂. e) Linker conformations of L-SO₂ (C_{2v} symmetry) in the confined framework of PCN-905-SO₂. f) Illustration of open pockets within the PCN-905-SO₂ structure and the large mesoporous channels formed by the assembly of RE₉ clusters and L-SO₂.

symmetry (Figure 2c,d). The 12-connected RE₉ clusters can be viewed as hexagonal prism nodes and the bent tetratopic linkers can be regarded as 4-connected joint triangular nodes. The overall structure was analyzed to be a 4,12-connected **dfs** net with a point symbol of {4⁴².6²⁴}{4⁶}₃ as determined by

TOPOS 4.0 (Figure 6b,c).^[22] Note that only four (4, 12)-edge transitive nets (**ftw**, **ith**, **shp** and **tam**) have been previously reported and this study uncovers a novel topology (**dfs**) constructed from 12-connected clusters and 4-connected linkers.

In the structure of PCN-905-SO₂, each two neighboring RE₉ clusters are parallel to each other and the assembly of these clusters leads to the formation of two types of channels. It contains large 1D open channels, with a diameter of 2.2 nm (Figure 2 f). Noticeably, the linkers are forced into a confined configuration with a 104.3° dihedral angle between the two central phenyl rings, and a 55.8° dihedral angle between the central phenyl ring and the two peripheral ones (Figure 2 e).

Interestingly, the underlying **dfs** topology of PCN-905-SO₂ can be viewed as an evolved network from **aea**-MOF-1 (Figure 3). The **aea**-MOF-1 reported by Eddaoudi and co-workers is built from 12-connected RE₉ clusters and 3-connected organic ligands (Figure 3 a).^[23] The **aea** net is

constructed from 2D layers pillared by 12-c RE₉ clusters, where the 2D layers are composed of the nonanuclear clusters arranged in a honeycomb (**hcb**) lattice pattern. The **hcb** layers are further intercalated by a periodic array of the 12-connected RE₉ clusters in the **aea** net while they are directly pillared by the bent tetratopic linkers without the participation of secondary RE₉ clusters as pillars in the **dfs** net (Figure 3 b). In other words, the **dfs** net can be viewed as an evolution process including the deconstruction of an **aea** net, pillar cluster elimination to generate a series of isolated **hcb** layers and subsequent direct reassembly of these **hcb** layers into the **dfs** net. Alternatively, the (4, 12)-c **dfs** net can also be viewed as an extended version of the (4, 6)-c **stp** net observed in PCN-600 with doubly linked linkers.^[24]

When replacing the pivot group with an *-O-* unit, the linker symmetry can be altered and decreased to C₁ accordingly (Figure 4). In the case of PCN-905-SO₂ constructed from C_{2v} linkers, each linker was connected to four RE₉ clusters

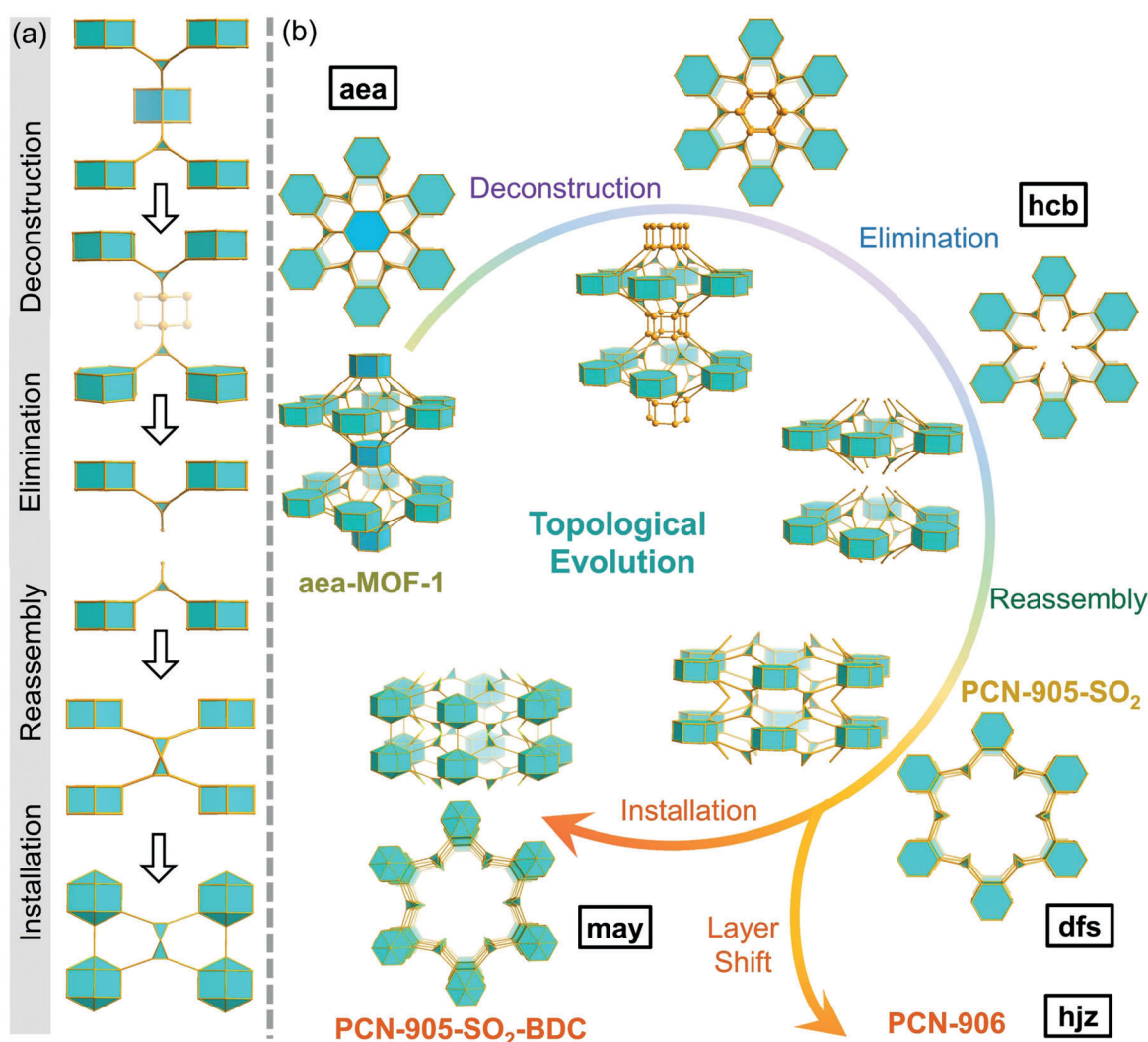


Figure 3. Stepwise topological evolution from an **aea** net to a **may** net via deconstruction, elimination, reassembly and installation processes.

a) The formation of a **may** net can be viewed as an evolution process including the deconstruction of a (3, 12, 12)-c **aea** net, pillar cluster elimination to generate a series of isolated **hcb** layers and subsequent direct reassembly of these **hcb** layers into the (4, 12)-c **dfs** net. Further installation of linear linkers generates a (4, 14)-c **may** net. b) Topological transformation pathway for the evolution from **aea**-MOF-1 to PCN-905-SO₂, and further to PCN-905-SO₂-BDC.

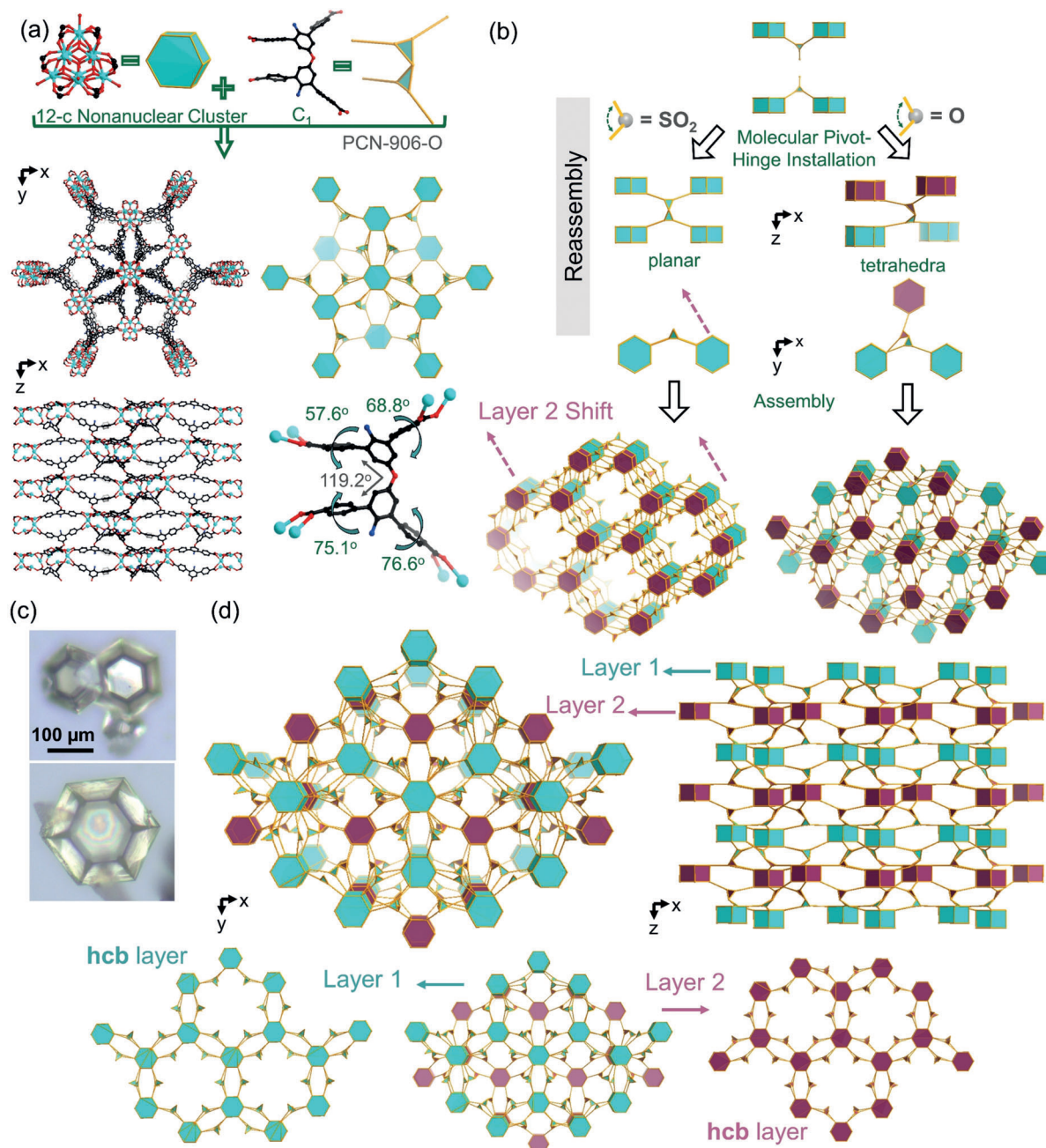


Figure 4. Structural illustration of PCN-906-O with a (4,12,12)-connected h_{1z} topology. a) The assembly of 12-c RE₉ clusters and 4-c ligands with an O pivot substituent (C₇) into a (4,12,12)-c h_{1z} net. The structural illustration of PCN-906-O and the simplified presentation of h_{1z} net were presented. b) Installation of a SO₂ pivot group leads to an eclipsed packing mode of hcb layers in PCN-905-SO₂, while a shift of RE₉ clusters was observed due to the linker configuration change, leading to a staggered stacking mode of these hcb layers in PCN-906-O. c) Optical images of PCN-906-O single crystals. d) Topological presentation of PCN-906-O with staggered hcb layer structures.

that are arranged in the same plane. However, when the linker configuration changes to a tetrahedral geometry, the arrangement of RE₉ clusters and the overall topology become more complicated. Solvothermal reactions between L-O and Eu(NO₃)₃·6H₂O in the presence of 2-fluorobenzoic acid (2-FBA) for 24 h yielded large colorless crystals with turtle-shell morphology, PCN-906-O (also named UPC-906-O, Figure 4c). However, these crystals shown only weak diffraction intensity, indicating that the organic components were highly disordered, although the RE metal clusters could be easily

distinguished. To illustrate the overall structure of PCN-906-O, we constructed a structural model based on the cluster locations and single crystal unit cell parameters (Figure S13). The phase purity of the aforementioned products was further accessed by PXRD patterns. PCN-906-O crystallized in the triclinic space group $P\bar{1}$. Crystallographically, it contains a 12-connected RE₉ cluster [RE₉(μ₃-OH)₁₂(μ₅-O)₂(O₂C-) ₁₂] as observed in PCN-905 and a bent tetratopic linker with C₇ symmetry (Figure 4a). The 12-connected RE₉ clusters can be viewed as hexagonal prism nodes, which are further con-

nected by a tetrahedra organic linker. The overall structure was analyzed to be a new (4,12,12)-connected **h_{jz}** net with a point symbol of $\{4^{24}, 6^{30}, 8^{12}\}\{4^{42}, 6^{24}\}\{4^6\}_6$ as determined by TOPOS 4.0 (Figure 4d).^[22] Note that the **h_{jz}** net can also be viewed as a pillared assembly of **h_{cb}** layers by the tetrahedra linker L-O. In PCN-905-SO₂, the **h_{cb}** layers adapt an eclipsed mode, therefore forming a mesoporous channel. However, in PCN-906-O, a shift of RE₉ clusters was observed due to the linker configuration change, leading to a staggered stacking mode of these **h_{cb}** layers (Figure 4b,d). The linker L-O in PCN-906-O exhibits a configuration with a 119.2° dihedral angle between the two central phenyl rings, while the dihedral angles between the central phenyl ring and the two peripheral rings vary from 57.6° to 76.6° (Figure 4a). Alternatively, the underlying **h_{jz}** net of PCN-906-O can be derived from a (4, 6, 6)-c net. For example, the construction of 6-connected triangular prism cluster and 4-connected linker lead to the formation of a novel **txs** net with a point symbol of $\{4^3, 6^{12}\}\{4^3, 6^3\}_3\{4^9, 6^6\}$ as determined by TOPOS 4.0 (Figure S16). After the linker insertion onto the 6-connected RE₉ clusters, the transformation from a **txs** net to a **h_{jz}** net can be accessed.

Modification of phenyl ring of L-CH₂ with bulky methyl groups can generate larger dihedral angle between the two hinges and force two peripheral phenyl rings perpendicular to the central one. Use of the bulky L-(CH₃)₆ ligand resulted in the discovery of PCN-908-(CH₃)₆ with **flu** topology built from newly discovered 8-c inorganic clusters (Figure 5a). Single-crystal X-ray analysis revealed that PCN-908-(CH₃)₆ crystallized in the triclinic space group *P* $\bar{1}$ (Figure 5b). It contains a novel 8-connected RE₆ cluster [RE₆(OH)₈(O₂C-)₉] and a tetratopic linker with C₁ symmetry (Figure 5d). Crystallographically, eight tetratopic linkers bridged four neighboring RE₆ clusters, which can be simplified into a (4, 8)-connected net with **flu** topology (Figure 5d). Topologically, the 8-connected metal clusters can be regarded as twisted cuboid nodes while the tetratopic linkers can be viewed as pivot-hinge nodes. The overall structure was analyzed to be a (4, 8)-connected net with a point symbol of $\{4^{12}, 6^{12}, 8^4\}\{4^6\}_2$.

The PCN-908-(CH₃)₆ framework here contains an unusual RE polynuclear clusters [RE₆(OH)₈(O₂C-)₈], where in the equatorial plane, only one oxygen from the carboxylate group on the linkers was coordinated to RE metals (Figure 5b). It should be noted that in the previously reported **flu**-MOFs such as PCN-605, a regular cuboid node without equatorial carboxylate coordination was usually observed.^[18] Due to the adaptable behaviors of RE clusters, when the linker configuration is altered, local missing-linker defects were found on the RE₆ cluster of PCN-908-(CH₃)₆, allowing for the formation of an extended ordered framework.

Noticeably, the addition of multiple bulky methyl substituents on the two central phenyl rings can generate much larger dihedral angles between the two central phenyl rings (117.2°) and between the central phenyl ring and the two peripheral rings (78.0–89.1°, Figure 5c). This result is consistent with our previous study on the steric effect of various functional groups, where -CH₃ groups tend to induce a larger torsion angle than -NH₂.^[19]

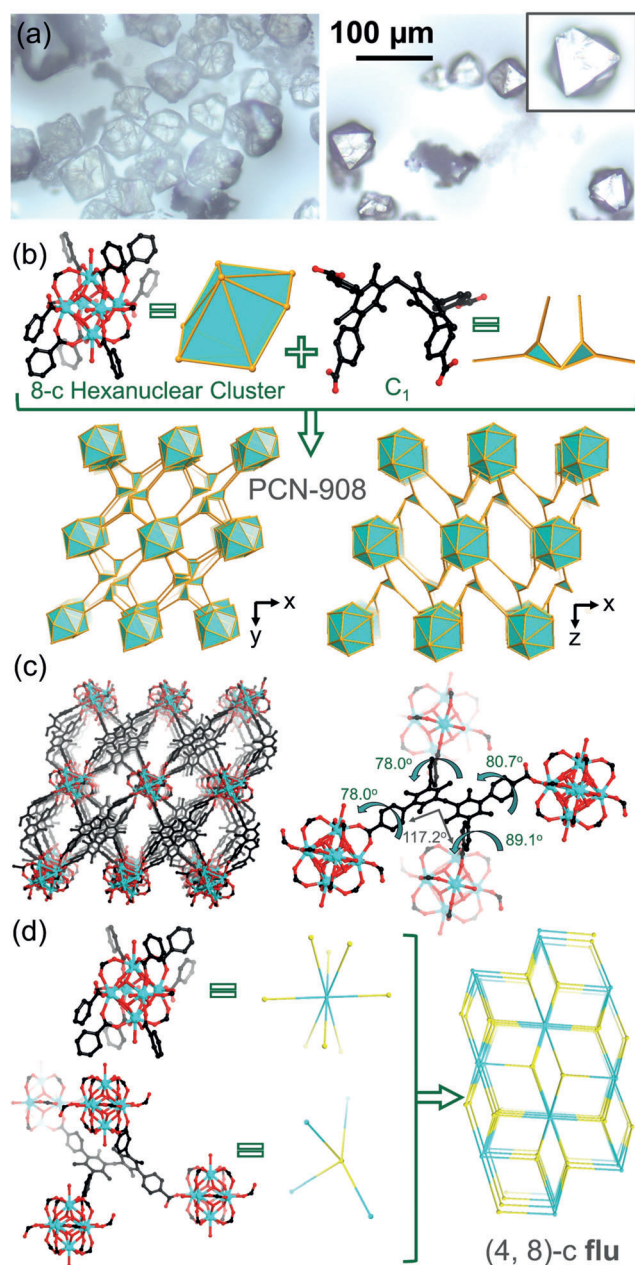


Figure 5. Structural illustration of PCN-908-(CH₃)₆ with a (4, 8)-c **flu** topology. a) Optical images of PCN-908-(CH₃)₆ single crystals. b) The assembly of 8-c RE₆ clusters and 4-c ligands with multiple bulky methyl groups (C₁) into a (4, 8)-c **flu** net. c) The structural illustration of PCN-908-(CH₃)₆. d) The simplified presentation of a (4, 8)-c **flu** network constructed from 8-connected RE metal nodes and 4-connected linker nodes.

Enhancing Diversity of RE-MOFs by Linker Installation

The flexible feature of the ligand and the defective nature of the RE cluster enable the precise placement of functional groups within a multivariate pore environment.^[25] For instance, the connectivity of 12-c RE₉ clusters in the structure of PCN-905-SO₂ can be further increased to eighteen, as seen in the structure of **gea**-MOF-1 and PCN-918. The missing-linker defects in the open pocket therefore enables the insertion of

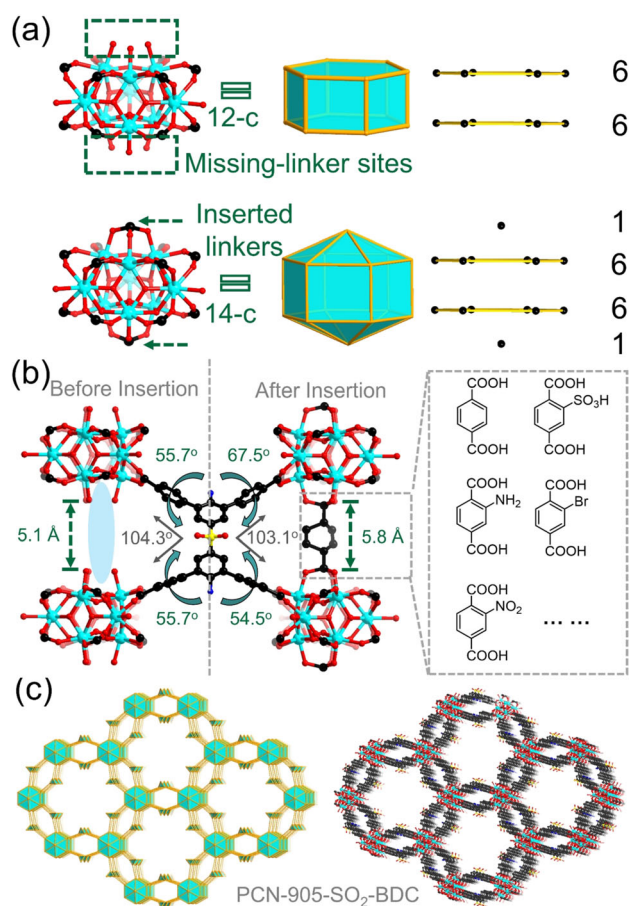


Figure 6. Structural illustration of PCN-905-SO₂-BDC with (4, 14)-c **may** topology. a) The hexagonal prism, representing 12-connected RE₉ clusters, can be extended to a new 14-connected RE₉ building block, by inserting one carboxylate moieties on the top and bottom side of the RE₉ clusters, respectively. A 14-connected RE₉ cluster with one hexagonal cone on the top and bottom side of the RE₉ clusters, respectively, was obtained. b) Structural illustration of PCN-905-SO₂ before and after installation of BDC linkers. The open pockets in PCN-905-SO₂ enables the precise placement of linkers with various functional groups within a multivariate pore environment. c) The illustration of **may** topology and PCN-905-SO₂-BDC structure.

linkers with various lengths and functionalities into the exposed RE sites (Figure 6a).^[26]

Considering the size of open pocket in the structure of PCN-905-SO₂, linear linkers including BDC and their functionalized versions BDC-A (A = -SO₃H, -NH₂, -Br and -NO₂) were chosen as precursors (Figure 6b). Solvothermal reactions between these linear linkers and PCN-905-SO₂ in the presence of DMF solvents for 24 h yielded large colorless crystals with cuboid morphology (Figure S11). There is no notable change on the morphology or volume after the linker installation as observed from optical images.

The structures of these installed RE-MOFs were further analyzed by single-crystal X-ray diffraction and the corresponding phase purity of the products was accessed by PXRD patterns (Figure S25). PCN-905-SO₂ inserted with BDC, PCN-905-SO₂-BDC, crystallized in the hexagonal space group *P6₃/mcm* (Table S1). Crystallographically, it contains a 14-connected RE₉ cluster [RE₉(μ₃-OH)₁₂(μ₃-O)₂(O₂C)₁₄],

a 2-connected linear linker and a 4-connected bent tetrapic linker with C_{2v} symmetry. The overall structure was found to be a 4,14-connected **may** net with a point symbol of {4⁵⁴.6³⁶.8}[4⁶]₃^[22] as determined by TOPOS 4.0 (Figure 6c).^[22]

It should be noted that the points of extension in the parent nonanuclear RE₉ cluster, originally linked by twelve carboxylates to form a hexagonal prism before installation, is increased to fourteen after insertion, with one carboxylate moiety inserted on each of the top and bottom side of the RE₉ clusters (Figure 6a). It should also be noted that the insertion of BDC linker slightly altered the unit cell parameters, the dihedral angle between the two central phenyl rings (from 104.3° to 103.1°), and the dihedral angle between the central phenyl ring and the two peripheral rings (from 55.7° from 54.5° or 67.5°, Figure 6b).

To further access the versatility of molecular pivot-hinge installation in RE-MOFs, PCN-905(RE) analogues with various RE metals (i.e., Eu, Y, Yb, Tb, Dy) have been successfully prepared under similar solvothermal reaction conditions, as indicated by PXRD patterns (Figure S18, 22). It should be noted that attempts to explore topologies of mixed-linker RE-MOFs by combining linkers with varying conformations were conducted, however, either pure MOFs doped with secondary linkers or MOF mixtures were obtained after solvothermal reactions.

Stability, Porosity and Catalytic Studies

The thermal stability of PCN-90X (RE, X = 5, 6 and 8) were analyzed by thermogravimetric analysis (TGA, Figure S30–34). The decomposition of PCN-90X(RE) starts at around 350°C, indicated by the weight loss of the corresponding organic linkers. In addition, the chemical stability of PCN-905(Eu)-SO₂ and PCN-905(Eu)-SO₂-BDC was examined by soaking the MOFs in various solvents for 24 h. PXRD patterns indicate that the PCN-905(Eu)-SO₂ and PCN-905(Eu)-SO₂-BDC have excellent chemical stability in most solvents, including DMF, acetone, CH₃OH and CH₂Cl₂ as evidenced by the well-maintained crystallinity (Figure S20, 23). PCN-905(Eu)-SO₂ shown relatively poor water stability, as observed by the broadened PXRD peaks after soaking in water for 24 h, due to the presence of open metal sites and lower connectivity number, while PCN-905(Eu)-SO₂-BDC exhibited improved water stability when exposed to water. The permanent porosity of the PCN-90X(RE) series was confirmed by N₂ sorption isotherms measured at 77 K (Figure S26–S29).

The open pockets in PCN-905-SO₂ enable the precise placement of functional groups within a multivariate pore environment. Taking advantage of the mesoporous nature and tailored pore environment of RE-based PCN-905-SO₂, linkers containing Brønsted acidic sites were post-synthetically anchored on the coordinatively unsaturated RE sites. This acid functionality can work in tandem with basic -NH₂ units installed on the pivot hinge linker to perform efficient cascade catalytic transformations within the functionalized channels (Figure 7).^[27–29] This system avoids the inefficiency observed with homogeneous systems wherein the acid and

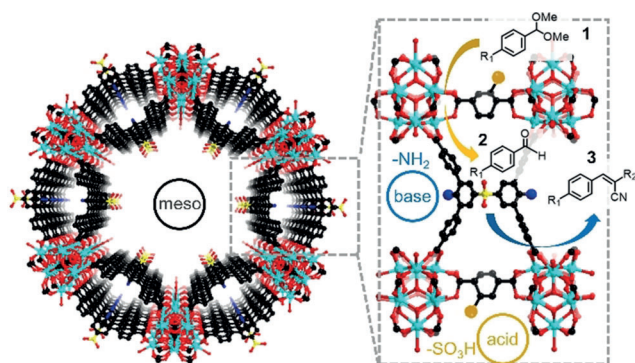


Figure 7. One-pot tandem reaction of benzaldehyde dimethylacetal and malononitrile by bifunctional mesoporous PCN-905(Eu)-SO₂-SO₃H catalyst.

base catalytic sites neutralize each other. By treating amino-functionalized PCN-905-SO₂ with a secondary acidic linker BDC-SO₃H, a bifunctional acid-base mesoporous catalyst was obtained and studied for its activity and recyclability in a tandem deprotection–aldol reaction, hydrolysis of an acetal and a Knoevenagel condensation.

The bifunctional PCN-905-SO₂-SO₃H quantitatively converts **1** to **2** after 1 h, as determined by gas chromatography, while product **3** is obtained with 95.5% yield. The remaining 4.5% of the final reaction mixture was identified as the intermediate benzaldehyde **2** (Table S4, entry 2). This demonstrates the high activity and selectivity of the tandem reaction. The high activity and selectivity was well-maintained across three catalytic cycles (Table S4, entry 2–4). In contrast, the use of PCN-905-SO₂ without inserted acidic ligands does not lead to the full conversion of reactants, only achieving 54.7% conversion of **1** and a 52.1% yield of **3** (Table S4, entry 1). The partial hydrolysis of **1** that was observed is likely promoted by the Lewis acidic RE centers, however the low conversion should be attributed to the lack of strong acid sites within the PCN-905-SO₂. The bifunctional catalyst can also convert reactants with various functional groups to **3** with high conversion and yield percentage (Table S4, entries 5 and 6).

Conclusion

In conclusion, we report a design strategy, molecular pivot-hinge installation, to prepare RE-MOFs with novel topologies and enhanced diversity. Depending on the compositions of the pivot groups and the sizes of linker substituents, various linker rotamers can be generated with a range of geometries and conformations. The combination of -SO₂- or -CH₂- functionalized linkers (L-SO₂ and L-CH₂) with C_{2v} symmetry and the 12-connected RE₉ clusters led to the formation of a new fascinating (4, 12)-c **dfs** topology, while the choice of a tetrahedra linker L-O leads to the discovery of a novel **hgz** topology with a staggered stacking mode. Additionally, the linked RE₆ clusters with a bulkier linker [(L-(CH₃)₆)] with C₁ symmetry gave rise to a (4, 8)-c **flu** topology. More interestingly, post-synthetic installation of linkers with

various functional groups in PCN-905-SO₂ enables the precise functionalization of the pore environment. Functionalization of each linker with acidic units and basic units in the mesoporous RE-based PCN-905-SO₂ allows the efficient cascade catalytic transformation of benzaldehyde dimethylacetal within the functionalized channels. This work provides novel design strategies for the systematic design and construction of unprecedented topologies through molecular pivot-hinge installation, which will further guide the discovery of periodic porous framework structures with intrinsic cooperativity.

Acknowledgements

This work was financially supported by the National Natural Science Foundation of China (NSFC Grant Nos. 21875285, 21571187), Taishan Scholar Foundation (ts201511019). The gas adsorption–desorption studies of this research were supported as part of the Center for Gas Separations, an Energy Frontier Research Center funded by the U.S. Department of Energy, Office of Science, Basic Energy Sciences under Award Number DE-SC0001015. The PXRD characterization and analysis were funded by the Robert A. Welch Foundation through a Welch Endowed Chair to H.-C.Z. (A-0030). We gratefully acknowledge Prof. Michael O’Keeffe for the help and insightful discussion.

Conflict of interest

The authors declare no conflict of interest.

Keywords: heterogeneous catalysis · linker desymmetrization · metal–organic frameworks · structural evolution · topology

- [1] S. Yuan, L. Feng, K. Wang, J. Pang, M. Bosch, C. Lollar, Y. Sun, J. Qin, X. Yang, P. Zhang, Q. Wang, L. Zou, Y. Zhang, L. Zhang, Y. Fang, J. Li, H. C. Zhou, *Adv. Mater.* **2018**, *30*, 1704303.
- [2] H. C. Zhou, J. R. Long, O. M. Yaghi, *Chem. Rev.* **2012**, *112*, 673–674.
- [3] A. Kirchon, L. Feng, H. F. Drake, E. A. Joseph, H. C. Zhou, *Chem. Soc. Rev.* **2018**, *47*, 8611–8638.
- [4] J. Lee, O. K. Farha, J. Roberts, K. A. Scheidt, S. T. Nguyen, J. T. Hupp, *Chem. Soc. Rev.* **2009**, *38*, 1450–1459.
- [5] M. Eddaoudi, J. Kim, N. Rosi, D. Vodak, J. Wachter, M. O’Keeffe, O. M. Yaghi, *Science* **2002**, *295*, 469–472.
- [6] S. M. Cohen, *Chem. Rev.* **2012**, *112*, 970–1000.
- [7] M. Li, D. Li, M. O’Keeffe, O. M. Yaghi, *Chem. Rev.* **2014**, *114*, 1343–1370.
- [8] E. A. Dolgoplova, A. J. Brandt, O. A. Ejegbavwo, A. S. Duke, T. D. Maddumapatabandi, R. P. Galhenage, B. W. Larson, O. G. Reid, S. C. Ammal, A. Heyden, *J. Am. Chem. Soc.* **2017**, *139*, 5201–5209.
- [9] L. Feng, K.-Y. Wang, G. S. Day, H.-C. Zhou, *Chem. Soc. Rev.* **2019**, *48*, 4823–4853.
- [10] Y. Bai, Y. B. Dou, L. H. Xie, W. Rutledge, J. R. Li, H. C. Zhou, *Chem. Soc. Rev.* **2016**, *45*, 2327–2367.

Research Articles

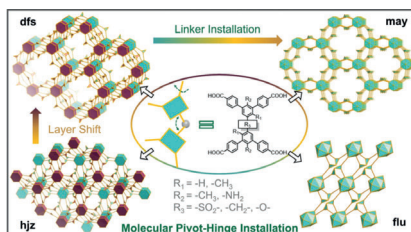
VIP

Metal–Organic Frameworks



L. Feng, Y. Wang, K. Zhang, K.-Y. Wang,
W. Fan, X. Wang, J. A. Powell, B. Guo,
F. Dai, L. Zhang, R. Wang, D. Sun,*
H.-C. Zhou*     

Molecular Pivot-Hinge Installation to
Evolve Topology in Rare-Earth Metal–
Organic Frameworks



Molecular pivot-hinge installation is introduced as a linker desymmetrization strategy to evolve the topology of rare-earth metal–organic frameworks (MOFs), where a pivot group is placed in the center of a linker similar to a hinge. By tuning the composition of pivot groups and steric hindrances of the substituents on various linker rotamers, MOFs with various topologies can be obtained.